Fabrication and Characterization of Advanced Triple-junction Amorphous Silicon Based Solar Cells

PHASE III – Quarter 1

Quarterly Technical Progress Report

March 1, 2007 to May 31, 2007

NREL Subcontract No. ZXL-5-44205-06

Subcontractor: The University of Toledo

Principal Investigator: Xunming Deng
(419) 530-4782; dengx@physics.utoledo.edu

Co-Principal Investigator: Robert W. Collins
(419) 530-2195; rcollins@physics.utoledo.edu

Department of Physics and Astronomy
University of Toledo, Toledo, OH 43606

Contract technical monitor: Dr. Bolko von Roedern

Table of Contents

Cover Page

Table of Contents

Section 1: Executive Summary

Section 2: Fabrication and optimization of a-Si:H n-i-p single-junction solar cells with 8 Å/s intrinsic layers of protocrystalline Si:H materials

Section 3: Advanced Deposition Phase Diagrams for Guiding Si:H-Based Multijunction Solar Cells

Section 1

Executive Summary

This quarterly technical progress report covers the highlights of the research activities and results on the project of "The Fabrication and Characterization of High-efficiency Triple-junction a-Si Based Solar Cells" at the University of Toledo for the Period of March 1, 2007 to May 31, 2007, under NREL TFPPP subcontract number ZXL-5-44205-06.

Following this Executive Summary are the sections performed during this quarter related to the tasks under this subcontract. The major technical progresses of these sections are summarized as follows:

Section 2: Fabrication and optimization of a-Si:H n-i-p single-junction solar cells with 8 Å/s intrinsic layers of protocrystalline Si:H materials

At the University of Toledo (UT), we have investigated hydrogenated amorphous silicon (a-Si:H) n-i-p solar cells with intrinsic layers deposited at high rates, ~ 8 Å/s, using a multi-chamber load-locked PECVD system. a-Si:H i-layers were grown with a VHF plasma density of ~ 0.2 W/cm^2 and a frequency of 70 MHz using various hydrogen dilution levels. It is observed from the current-voltage (I-V) device performance characteristics that the open-circuit voltage (V_{oc}) increases with increasing hydrogen dilution, reaches a maximum, and then decreases. This drop in V_{oc} can be attributed to the transition region (or protocrystalline regime) from an amorphous phase into a mixed amorphous+nanocrystalline (a + nc) phase for the i-layer. An initial efficiency of η = 9.99% (V_{oc} = 0.986 V, J_{sc} = 13.98 mA/cm^2, FF = 72.5%) was obtained. Quantum efficiency (QE) measurement has shown that the blue light response increases as the hydrogen dilution increases. High blue light spectral response with QE values over 0.7 at λ = 400 nm has been obtained for a-Si:H cells made under specific deposition conditions in which tailored protocrystalline silicon materials were incorporated at the i/p interface region. A stabilized efficiency of ~ 8.2% has been achieved for the cells with protocrystalline or (a+nc)-mixed Si:H of a small portion being evolved at the top-most i-layer near p/i interface.

Section 3: Advanced Deposition Phase Diagrams for Guiding Si:H-Based Multijunction Solar Cells

Phase diagrams have been established to describe very high frequency (vhf) plasma-enhanced chemical vapor deposition (PECVD) processes for intrinsic hydrogenated silicon (Si:H) and silicon-germanium alloy ($Si_{1-x}Ge_x$:H) thin films using crystalline Si substrates that have been over-deposited with n-type amorphous Si:H (a-Si:H). The Si:H and $Si_{1-x}Ge_x$:H processes are applied for the top and middle i-layers of triple-junction a-Si:H-based n-i-p solar cells fabricated at University of Toledo. Identical n/i cell structures were co-deposited on textured Ag/ZnO back-reflectors in order to correlate the phase diagram and the performance of single-junction solar cells, the latter completed through over-deposition of the p-layer and top contact. This study has reaffirmed that the highest efficiencies for a-Si:H and a-$Si_{1-x}Ge_x$:H solar cells are obtained when the i-layers are prepared under maximal H_2 dilution conditions.

Section 2

Fabrication and optimization of a-Si:H n-i-p single-junction solar cells with 8 Å/s intrinsic layers of protocrystalline Si:H materials

Xinmin Cao, Wenhui Du, Yasuaki Ishikawa, Xianbo Liao, Robert W. Collins, Xunming Deng
Department of Physics and Astronomy, University of Toledo, Toledo, OH 43606, USA

ABSTRACT

At the University of Toledo (UT), we have investigated hydrogenated amorphous silicon (a-Si:H) n-i-p solar cells with intrinsic layers deposited at high rates, ~ 8 Å/s, using a multi-chamber load-locked PECVD system. a-Si:H i-layers were grown with a VHF plasma density of ~ 0.2 W/cm^2 and a frequency of 70 MHz using various hydrogen dilution levels. It is observed from the current-voltage (I-V) device performance characteristics that the open-circuit voltage (V_{oc}) increases with increasing hydrogen dilution, reaches a maximum, and then decreases. This drop in V_{oc} can be attributed to the transition region (or protocrystalline regime) from an amorphous phase into a mixed amorphous+nanocrystalline (a + nc) phase for the i-layer. An initial efficiency of η = 9.99% (V_{oc} = 0.986 V, J_{sc} = 13.98 mA/cm^2, FF = 72.5%) was obtained. Quantum efficiency (QE) measurement has shown that the blue light response increases as the hydrogen dilution increases. High blue light spectral response with QE values over 0.7 at λ = 400 nm has been obtained for a-Si:H cells made under specific deposition conditions in which tailored protocrystalline silicon materials were incorporated at the i/p interface region. A stabilized efficiency of ~ 8.2% has been achieved for the cells with protocrystalline or (a+nc)-mixed Si:H of a small portion being evolved at the top-most i-layer near p/i interface.

INTRODUCTION

A high V_{oc} and a high spectral response in the short wavelength region are desired for the hydrogenated amorphous silicon (a-Si:H) n-i-p solar cell, which has a wide bandgap E_g of ~1.8 eV and normally serves as a window top-cell in the a-Si based multi-junction solar cell [1].

A detailed phase diagram describing hydrogenated silicon materials, including (i) purely amorphous silicon, a-Si:H, (ii) protocrystalline Si:H, (iii) mixed amorphous+micro (or amorphous+nano) crystalline silicon, (a + μc)-Si:H [or (a + nc)-Si:H], and (iv) single-phase micro- (or nano-) crystalline silicon, μc-Si:H (or nc-Si:H) have been developed by Wronski and Collins *et al.* [2, 3]. The protocrystalline Si:H materials are more ordered than conventional a-Si:H materials and evolve with thickness from an amorphous phase into first an (a+nc)-Si:H mixed-phase and subsequently into nc-Si:H, a fully nanocrystalline phase. Such silicon materials at the transition regime between the amorphous phase and the (a+nc)-Si:H mixed-phase can be defined as protocrystalline silicon.

For the fabrication and optimization of a-Si:H solar cells, the properties and growth conditions of protocrystalline Si:H materials are of great interest. The materials made in the protocrystalline regime contain a predominant amorphous component possibly with a very small volume fraction of nano-crystalline inclusions and as a result exhibit unique optoelectronic properties. By further understanding and developing Si:H deposition phase diagrams, we can fabricate and optimize high quality a-Si materials and high performance solar cells in a more controlled way.

The VHF PECVD technique along with H_2 dilution grading processes have been applied in our laboratory in the fabrication of a-Si based solar cells at deposition rates in the range 2 ~ 40 Å/s. In the research reported here, we investigated a-Si:H n-i-p solar cells with intrinsic layers deposited at a high deposition rate of ~8 Å/s. By adjusting the i-layer deposition conditions, such as the H_2 dilution ratio and H_2 dilution grading profile, a-Si:H solar cells have incorporated protocrystalline materials near the amorphous/nanocrystalline transition. The device performance of the a-Si:H solar cells have been greatly improved as a result.

EXPERIMENT

a-Si:H n-i-p single-junction solar cells were fabricated using PECVD techniques in our UT multi-chamber load-locked deposition system. The substrates were stainless steel (SS) coated with Ag/ZnO back reflectors. The Si:H i-layers were prepared at a high deposition rate of ~ 8 Å/s using the VHF-PECVD technique with a frequency of 70 MHz, a plasma density of ~ 0.2 W/cm^2, and under a low deposition pressure region. As a result, the deposition time for an a-Si:H i-layer was about 5 minutes, corresponding to a thickness of ~ 240 nm. The nominal substrate temperature T_{sub} was in the range of 100 – 300 °C. A high hydrogen dilution ratio R=[H_2]/[Si_2H_6] in the range of 30 – 100 has been used for i-layer deposition. The doped n and p layers were prepared using the conventional 13.56 MHz RF-PECVD technique at deposition rates of 1 Å/s under amorphous and protocrystalline growth conditions, respectively [4]. After fabrication of the n-i-p single-junction structure, the cells were completed by depositing indium tin oxide (ITO) transparent conductive layers through a mask to serve as the front contacts. Standard RF magnetron sputtering deposition techniques were used for the ITO. Each cell has an active area of 0.25 cm^2. For characterization of the as-deposited cells, standard dark current-voltage (I-V) and AM1.5G light I-V measurements were made. Standard QE measurements were made in the wavelength range of 350 – 1000nm. Light-soaking experiments were undertaken with ~ 100 mW/cm^2 white light at 50 °C.

RESULTS AND DISCUSSIONS

It is well known that hydrogen dilution can strongly influence a-Si:H based solar cell performance [5, 6]. In particular, the open-circuit voltage (V_{oc}) increases gradually with an increase in hydrogen dilution and reaches a maximum value of ~ 1.0 V, where protocrystalline material is believed to be present. Normally, for protocrystalline material there is no indication of a crystalline component in the ellipsometry and Raman spectra; however, through TEM one can detect a small crystalline component in the films deposited under conditions very close to the transition [3, 4]. If the hydrogen-dilution exceeds a certain level, (a + nc)-Si:H mixed-phase materials and solar cells can be made, and the corresponding V_{oc} values start to drop. By increasing hydrogen dilution even further, a V_{oc} value around 0.5 V can be attained -- a typical value for nc-Si:H solar cells [7].

So we can evaluate the structural phase information at the top of the as-grown i-layers simply from the V_{oc} value and its trend for the corresponding actual solar cells. We have used high hydrogen dilution ratios R in the range of 30 – 100 for a series of i-layers focusing on the protocrystalline phase in the transition region between a purely a-Si:H phase and an (a + nc)-Si:H mixed-phase. Meanwhile, a specific hydrogen dilution grading approach has been applied for the i-layer deposition, designed so that optimum protocrystalline silicon materials are incorporated at the i/p interface region.

Table I displays the AM1.5G device I-V performance characteristics in the initial state and after 100 hours of light soaking for a-Si:H n-i-p single-junction solar cells on Ag/ZnO back reflector coated stainless steel substrates. The 240 nm-thick i-layer has been made by 70 MHz VHF-PECVD with a deposition rate of 8 Å/s and a deposition time of 5 minutes. An average initial active-area efficiency of ~ 9.6% has been obtained for the a-Si:H cells of sample GD1828.

Table I. I-V and QE data in the initial state and after 100 hours of light soaking for 8 Å/s VHF a-Si:H n-i-p solar cells made on Ag/ZnO coated SS substrate.

Cell Nr.		V_{oc} (V)	J_{sc} (mA/cm^2)	QE @ λ = 400 nm	FF (%)	η (%)	comments
GD1828-2.51 (near gas inlet)	initial	0.946	14.97	0.591	65.2	9.23	upstream side
	100 hrs LS	0.922	14.73	0.542	59.3	8.05	
	degradation (%)	*-2.5*	*-1.6*	*-8.3*	*-9.0*	***-12.8***	
GD1828-2.31	initial	0.967	14.38	0.602	69.2	9.62	
	100 hrs LS	0.943	14.14	0.577	63.7	8.49	
	degradation (%)	*-2.5*	*-1.7*	*-4.2*	*-7.9*	***-11.7***	
GD1828-2.11 (center)	initial	**0.986**	**13.98**	**0.600**	**72.5**	**9.99**	
	100 hrs LS	0.962	13.75	0.586	66.8	**8.84**	
	degradation (%)	*-2.4*	*-1.6*	*-2.3*	*-7.9*	***-11.6***	
GD1828-4.11 (center)	initial	0.968	13.69	0.633	73.8	9.78	down-stream side
	100 hrs LS	0.956	13.50	0.627	67.8	8.75	
	degradation (%)	*-1.2*	*-1.4*	*-0.9*	*-8.1*	***-10.5***	
GD1828-4.12	initial	0.954	13.76	0.664	72.8	9.56	
	100 hrs LS	0.950	13.64	0.654	67.9	8.80	
	degradation (%)	*-0.4*	*-0.9*	*-1.5*	*-6.7*	***-7.9***	
GD1828-4.13	initial	0.938	14.12		71.8	9.51	
	100 hrs LS	0.939	14.00	0.690	67.0	8.81	
	degradation (%)	*0.1*	*-0.8*		*-6.7*	***-7.4***	
GD1828-4.14 (near pumping outlet)	initial	0.927	14.37	0.737	70.9	9.44	
	100 hrs LS	0.932	14.20	0.722	66.3	8.77	
	degradation (%)	*0.5*	*-1.2*	*-2.0*	*-6.5*	***-7.1***	

It should be noted that the gas feeding and pumping system has a cross-flow configuration in the present i-layer deposition chamber whereby the Si_2H_6 and H_2 gases enter from one side port of the chamber and exit from the opposite side port with gases flowing across the 4" x 4" substrate. This i-layer chamber has been used for routine fabrication of a-Si:H based cells using conventional RF PECVD at rates less than 2 Å/s and has yielded relatively good uniformity not only in the thickness and phase structure of the material but also in the device performance. However, this cross-flow configuration results in a non-uniformity of ~ ±10% in film thickness across the 4" x 4" substrate under the high rate deposition conditions of ~ 8 Å/s.

The AM1.5 light and dark I-V plots of the best a-Si cell of 9.99% initial efficiency (V_{oc}= 0.986 V, J_{sc}= 13.98 mA/cm^2, and FF=0.725) are displayed in Fig 1. This best cell is located at the upstream side near the sample center having a i-layer thickness of 220 nm with a deposition rate of 7.3 Å/s. Figure 2 plots the corresponding external quantum efficiency versus wavelength over the range of 380-1000 nm for cells whose I-V data are listed in Table I.

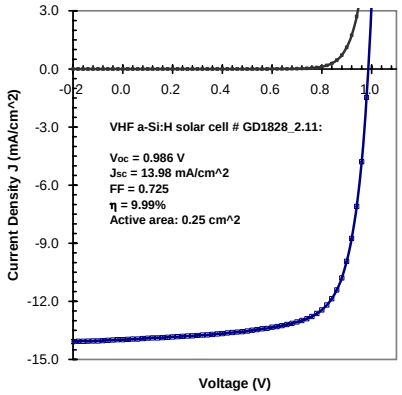

Fig. 1. AM1.5G light and dark I-V plots for a 7.3 Å/s VHF a-Si solar cell on Ag/ZnO BR.

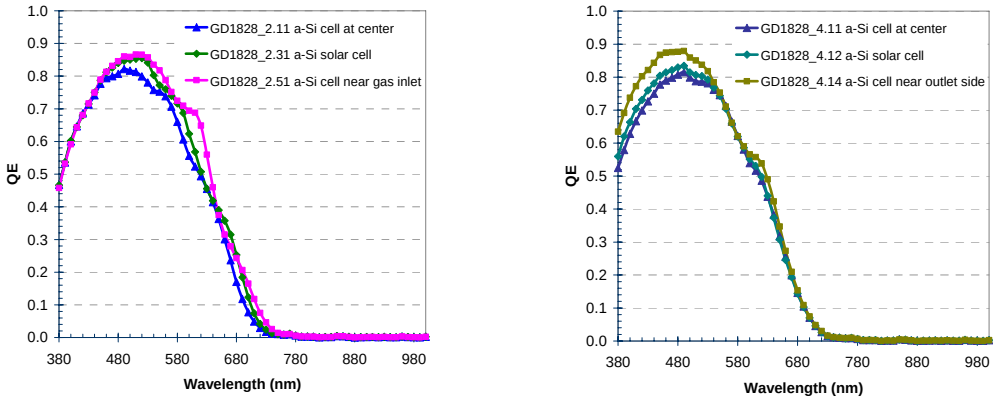

(a) (b)

Fig. 2. External quantum efficiency plots for 8 Å/s VHF PECVD a-Si solar cells on Ag/ZnO BR: a) cells on the upstream side, and b) cells on the downstream side.

The V_{oc} values of the solar cells with i-layers made in the protocrystalline regime are very sensitive to the hydrogen dilution. For the sample GD1828 shown in Table I, the device performance characteristics show clear differences for solar cells fabricated across the substrate between the upstream side (near the gas inlet port) and the downstream side (near the outlet pumping port). These differences reflect underlying structural and thickness variations for the as-grown i-layer across the substrate. Starting at a V_{oc} value of 0.946 V for the solar cell nearest the gas inlet side, the V_{oc} values increase with cell position across the substrate, reach a maximum value of 0.986 V for the cell in the center, and then decrease to a minimum V_{oc} value of 0.927 V for the cell nearest to the outlet side. This behavior indicates that there is an obvious non-uniformity in H_2 dilution across substrate because of the high consumption of silicon atoms at high deposition rates. Thus, the structural phase of the as-grown i-layer changes from a purely amorphous phase for cells at the upstream side with relatively low H_2 dilution, to the protocrystalline regime for cells at the sample center with moderate H_2 dilution, and subsequently to an (a+nc)-Si:H mixed-phase for cells at the downstream side with higher H_2 dilution than that near the gas inlet. Based on the above analysis, we can easily interpret I-V and QE results for the cells as functions of H_2 dilution rather than cell position across the substrate. Thus, we can reveal the typical device performance behavior as a function of H_2 dilution instead of cell position for a-Si solar cells fabricated in a single run in the same way as those from a series of a-Si cell depositions with H_2 dilution variations from deposition to deposition.

For the initial device performance characteristics among the set of solar cells along gas flow direction, the cell GD1828-2.51, which is at the position nearest to the gas inlet, has the highest J_{sc} of 14.97 mA/cm^2. There are two major reasons contributing to the highest J_{sc}. One reason is that this cell has the thickest i-layer of d = 240 nm; the second reason is that the cell incorporates a pure a-Si i-layer of the lowest band gap and thus has the highest light absorption and QE in the long wavelength range of 550 – 750 nm (as shown in Fig. 2a).

The cell GD1828-4.11 in the sample center has the best initial state FF of 0.738, but the lowest J_{sc} of 13.69 mA/cm^2 due in part to the lower i-layer thickness of 220 nm. For cells on the downstream side near the pumping outlet, the i-layer thickness decreases further from 220 nm to 200 nm. In spite of this, however, the J_{sc} increases from 13.69 to 14.37 mA/cm^2. As shown in Fig. 2b, the increase in J_{sc} mainly arises from the increase in blue QE in the short wavelength range of 380 – 480 nm, whereas the spectral responses remain about same in the long wavelength range of 550 – 750 nm. The latter similarity arises because the i-layers are protocrystalline materials with about same wide optical bandgap. The cell GD1828_4.14, being the nearest to the pumping outlet side, has the lowest V_{oc} of 0.927V whereby a small portion of (a+nc)-Si:H mixed-phase is evolved at the top-most i-layer near the i/p interface. High blue light spectral responses with QE values over 0.7 at λ = 400 nm have been obtained here. There are two key reasons for the increase in blue QE for the cells on the downstream side of the center. One is the presence of improved protocrystalline material in the bulk i-layer characterized by improved mobility of the photo-generated carriers and reduced recombination. The second is the reduced absorption in the window p-layer possibly due to the presence of small nanocrystallites. When using the standard protocrystalline Si:H p-layer deposition condition for these a-Si solar cells, the as-grown p-layer becomes more transparent, especially for blue light, when it is deposited on the protocrystalline i-layer near the boundary of the transition to (a+nc)-Si:H growth.

After 100 hours of light soaking, all cells have only small drops of 1-2% in J_{sc}. For cells along the gas flow direction, with the increase of H_2 dilution, the light-induced degradation in FF is reduced from 9% to 6.5%, meanwhile the degradation in V_{oc} is also reduced. The cell GD1828_4.14, being nearest to the pumping outlet side, even exhibits an increase of 5 mV in V_{oc} after 100 hrs of light soaking. Consequently, cells prepared with higher H_2 dilution exhibit greater stability in efficiency. Moreover, the smaller thickness should also be one of the reasons for the lower degradation.

For the stability study, a prolonged light soaking of 5000 hours has also been taken to this sample. Figure 3 plots a comparison of cell efficiencies as functions of cell position for the initial state, 100 hours, and 5000 hours of light soaking, where the cell position means the distance between the measured solar cell and the sample upstream edge near the gas inlet. A most stabilized efficiency of ~ 8.2% has been achieved for the downstream cells with protocrystalline or (a+nc)-mixed Si:H of a small portion being evolved at the top-most i-layer near p/i interface. But only a 7.35% efficiency was obtained for the cell with purely amorphous Si:H bulk i-layer being the nearest to the gas inlet. The degradation ratio in efficiency decreases from 20.4% for the cell near the gas inlet to 13.2% for the cell near the pumping outlet.

Finally, it should be noted that the highest stabilized performance of V_{oc}, FF, and J_{sc} occurs at different H_2 dilution levels across the substrate area. If we were to ascribe the dominant contributor to the maximum V_{oc} to the i/p interface, the FF to the bulk i-layer, and J_{sc} to a combination of the bulk i-layer (enhanced hole diffusion length and reduced recombination) and p-layer transparency, then a new multistep approach with substrate memory erasing regions and crystallite enhancing regions may be proposed to achieve these maxima in a single device.

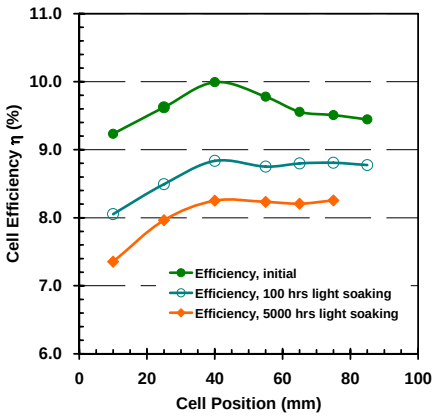

Fig. 3. A comparison of cell efficiencies as functions of cell position for the initial state, 100 hours, and 5000 hours light soaking.

CONCLUSIONS

Using a Si:H deposition phase diagram as guidance, we have fabricated and optimized high performance single-junction a-Si:H n-i-p solar cells with 8 Å/s intrinsic layers of protocrystalline Si:H materials. We have found that the V_{oc} values of the solar cells with i-layers made near the protocrystalline regime are very sensitive to the hydrogen dilution ratio $R=[H_2]/[Si_2H_6]$. An initial efficiency of η = 9.99% was obtained for the cell with improved protocrystalline silicon material evolved at the i/p interface region. The light-induced stability in efficiency is improved for cells with protocrystalline materials or (a+nc)-mixed Si:H of a small portion being evolved at the top-most i-layer near i/p interface. High blue light spectral response with QE values over 0.7 at λ = 400 nm has been obtained here. A stabilized efficiency of ~ 8.2% has been achieved after 5000 hours of light soaking.

ACKNOWLEDGMENTS

This work was supported by the National Renewable Energy Laboratory "Thin Film Photovoltaic Partnership Program" under subcontract No. ZXL-5-44205-06.

REFERENCES

1. X. Deng and E. Schiff, a chapter in *The Handbook of Photovoltaic Science and Engineering*, edited by A. Luque & S. Hegedus, (John Willey & Sons, Ltd., 2003).
2. C. R. Wronski and R. W. Collins, *Solar Energy* **77**, 877-885 (2004).
3. R. W. Collins, A. S. Ferlauto, G. M. Ferreira, C. Chen, J. Koh, R. J. Koval, Y. Lee, J. M. Pearce, and C. R. Wronski, *Solar Energy Materials & Solar Cells* **78**, 143 (2003).
4. W. Du, X. Liao, X. Yang, H. Povolny, X. Xiang, X. Deng, and K. Sun, *Solar Energy Materials and Solar Cells* **90,** 1098-1104 (2006).
5. B. Yan, J. Yang, G. Yue, and S. Guha, *2003 MRS Spring Meeting*, (San Francisco, CA; USA; 22-25 Apr. 2003), pp. 363-368 (2003).
6. S. Guha, J. Yang, A. Banerjee, B. Yan, and K. Lord, *Solar Energy Materials and Solar Cells* **78**, 329-347 (2003).
7. X. Cao, W. Du, X. Yang, and X. Deng, *4th World Conference on Photovoltaic Energy Conversion*, May 2006, Waikoloa HI (IEEE, Piscataway NJ, 2006).

Section 3

Advanced Deposition Phase Diagrams for Guiding Si:H-Based Multijunction Solar Cells

J.A. Stoke, N.J. Podraza, Jian Li, Xinmin Cao, Xunming Deng, and R.W. Collins
Department of Physics and Astronomy, University of Toledo, Toledo, OH 43606, USA

ABSTRACT

Phase diagrams have been established to describe very high frequency (vhf) plasma-enhanced chemical vapor deposition (PECVD) processes for intrinsic hydrogenated silicon (Si:H) and silicon-germanium alloy ($Si_{1-x}Ge_x$:H) thin films using crystalline Si substrates that have been over-deposited with n-type amorphous Si:H (a-Si:H). The Si:H and $Si_{1-x}Ge_x$:H processes are applied for the top and middle i-layers of triple-junction a-Si:H-based n-i-p solar cells fabricated at University of Toledo. Identical n/i cell structures were co-deposited on textured Ag/ZnO back-reflectors in order to correlate the phase diagram and the performance of single-junction solar cells, the latter completed through over-deposition of the p-layer and top contact. This study has reaffirmed that the highest efficiencies for a-Si:H and a-$Si_{1-x}Ge_x$:H solar cells are obtained when the i-layers are prepared under maximal H_2 dilution conditions.

INTRODUCTION

State-of-the-art solar cells based on a-Si:H prepared by PECVD employ a triple-junction design [1,2]. Optimization of the a-Si:H i-layer of the top cell has been widely successful through the concept of maximal H_2 dilution [3,4]. The benefits of H_2 dilution include enhanced surface passivation and hence diffusion of film precursors in the PECVD process, as well as enhanced relaxation of sub-surface strained Si-Si bonds [4]. The resulting "protocrystalline" nature of the i-layer provides the highest device performance and stability. In this study, vhf PECVD phase diagrams have been developed for Si:H and $Si_{1-x}Ge_x$:H i-layers deposited from Si_2H_6 + GeH_4 mixtures on a-Si:H n-layers under conditions used for high-efficiency triple-junction n-i-p cells. These diagrams have been correlated with single-junction cell performance in order to further explore and extend the applicability of the maximal H_2 dilution concept.

EXPERIMENTAL DETAILS

The Si:H and $Si_{1-x}Ge_x$:H i-layers for phase diagram development by real time spectroscopic ellipsometry (RTSE) were deposited on c-Si/(native-oxide)/(n-type a-Si:H) substrate structures using multichamber vhf (70 MHz) PECVD. Such substrates ensure a specular surface to aid in the utilization of RTSE [5] for the first time in the characterization of PECVD a-$Si_{1-x}Ge_x$:H from S_2H_6 and GeH_4. In order to apply deposition phase diagrams from RTSE for insights into n-i-p solar cell performance, additional samples ~2000 Å thick were co-deposited onto textured Ag/ZnO/(n-type a-Si:H) back-reflectors in the device configuration simultaneously with the specular c-Si/(native-oxide)/(n-type a-Si:H) substrates. For depositions performed versus the phase diagram variable $R=[H_2]/\{[Si_2H_6]+[GeH_4]\}$, all other parameters were selected as those used for the previously-optimized top and middle i-layers of a triple junction solar cell, including a vhf power of 8 W, a low source gas $[Si_2H_6]+[GeH_4]$ partial pressure of $p < 0.004$ Torr, a low total gas pressure of $p_{tot} \sim 0.2$ Torr, and nominal substrate temperatures of T=200°C for Si:H and T=350°C for $Si_{1-x}Ge_x$:H. These nominal values correspond to calibrated values of T=107°C and 170°C, respectively, determined by RTSE [6]. In order to produce the desired optical gaps, the flow ratio $G=[GeH_4]/\{[Si_2H_6]+[GeH_4]\}$ was set at G=0 for the top i-layer, resulting in growth rates ranging from ~2.3 to ~0.8 Å/s as R increases from 60 to 150, and G=0.286 for the middle i-layer, resulting in growth rates ranging from ~2.6 to ~1.1 Å/s as R increases from 45 to 150.

RESULTS

Figure 1 shows the optical band gaps plotted versus the H_2 dilution flow ratio R for the a-Si:H and a-$Si_{1-x}Ge_x$:H i-layers. These optical gaps were obtained from RTSE data collected at the deposition temperature after i-layer thicknesses of 150-250 Å, and were deduced both from extrapolations of $\varepsilon_2^{1/2}$ versus E (open circles) and from complete fits using a parameterized Cody-gap-modified Lorentz oscillator (solid squares) [7]. Both approaches are based on the assumptions of parabolic bands and a constant dipole matrix element. For a-Si:H films prepared over the range in R from 60 to150, gaps from 1.65 to 1.80 eV are observed. From R = 60 to 120, the band gap shows an increase with increasing R; however, from R=120 to 150 the gap is nearly constant. For a-$Si_{1-x}Ge_x$:H films prepared over the range in R from 45 to 150, gaps from 1.35 to 1.48 eV are observed with a continuous linear increase over the full range.

Figure 2 shows the surface roughness layer thickness versus the bulk layer thickness during Si:H growth with two H_2 dilution levels. Examples are provided for a Si:H film that remains amorphous throughout growth (R=60) and for one in which microcrystallites nucleate from the amorphous phase, grow preferentially, and coalesce to a single-phase microcrystalline structure (R = 150). In particular, the R=150 data reveal the amorphous-to-(mixed-phase microcrystalline) roughening transition, denoted a $\rightarrow$ (a+μc), and the (mixed-phase)-to-(single-phase) microcrystalline smoothening transition, denoted (a+μc) $\rightarrow$ μc. The latter films can be analyzed using a four-medium (pseudo-substrate/outer-layer/surface-roughness/ambient) virtual interface technique designed to extract the volume fraction of microcrystallites in the top ~10 Å of the bulk layer and thus to generate a depth profile in the microcrystalline fraction as shown in Fig. 3.

Similar data in the evolution of the roughness thickness and microcrystalline volume fraction were compiled for all Si:H films prepared versus R in order to establish the phase diagram in Fig. 4. This diagram demonstrates that, under the vhf PECVD conditions used here, the Si:H films remain amorphous throughout ~2000 Å of bulk layer growth for R ≤ 80. At higher H_2 dilution (100 ≤ R ≤ 150), the Si:H films initially nucleate as a-Si:H but undergo the a $\rightarrow$ (a+μc) transition at a thickness that decreases with increasing R. Figure 4 shows that the surface roughening

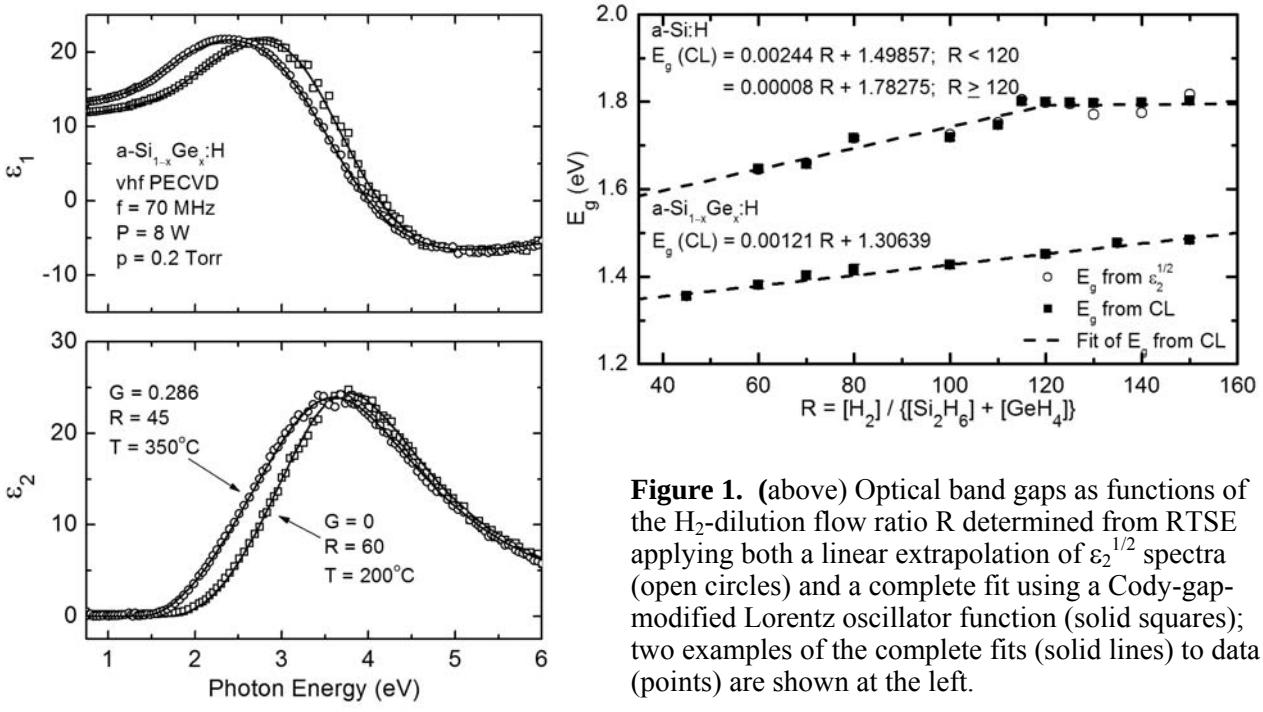

Figure 1. (above) Optical band gaps as functions of the H_2-dilution flow ratio R determined from RTSE applying both a linear extrapolation of $\varepsilon_2^{1/2}$ spectra (open circles) and a complete fit using a Cody-gap-modified Lorentz oscillator function (solid squares); two examples of the complete fits (solid lines) to data (points) are shown at the left.

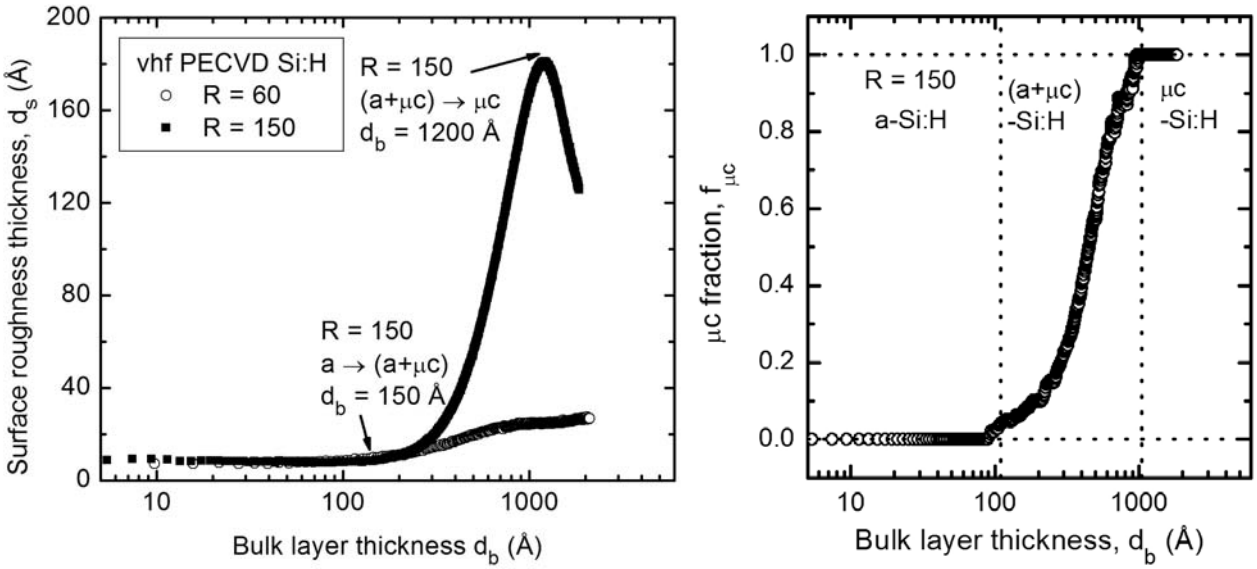

Figure 2 (left). Surface roughness evolution for a vhf PECVD Si:H film in the fully amorphous growth regime (R = 60) and one in the microcrystalline (μc) evolution regime (R = 150).
Figure 3 (right). The μc fraction in the top 10 Å of the bulk layer, determined from virtual interface analysis of RTSE data for the R = 150 Si:H film, plotted versus the accumulated bulk layer thickness.

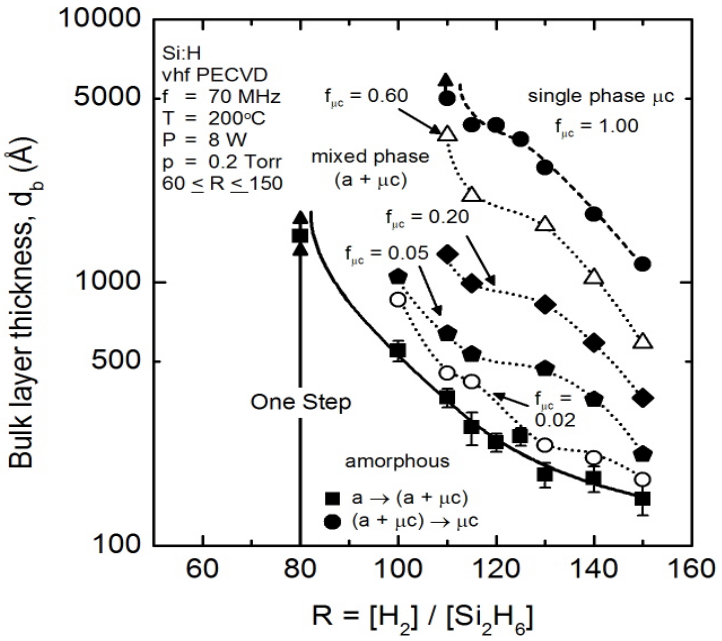

Figure 4. A deposition phase diagram for Si:H films prepared under vhf PECVD conditions. The bulk layer thicknesses at which the a → (a+μc) transition (solid line, squares), and the (a+μc) → μc transition (dashed line, circles) occur are depicted, as deduced from data such as those of Fig. 2. Up-arrows indicate that the transitions occur at thicknesses above the indicated values. Contour lines in the microcrystallite volume fraction $f_{\mu c}$ are plotted ranging from 0.02 to 0.60 (dotted lines). It is clear that the surface roughening effect provides sensitivity to the a → (a+μc) transition at microcrystallite volume fractions of better than 0.02 within the near-surface of the bulk layer.

effect as in the data for R=150 in Fig. 2 provides sensitivity to the a → (a+μc) transition at microcrystalline volume fractions of < 0.02 within the near-surface of the bulk layer.

The structural evolution of the $Si_{1-x}Ge_x$:H exhibits behavior analogous to that of the Si:H series with respect to the appearance of the a → (a+μc) and (a+μc) → μc transitions. The surface roughness and microcrystallite evolution data acquired for depositions at varying R were used to compile the vhf PECVD phase diagram in Fig. 5. This diagram demonstrates that, under the deposition conditions used here, films remain amorphous throughout ~2000 Å of bulk layer growth for R ≤ 70. At higher H_2 dilutions (80 ≤ R ≤ 150), the $Si_{1-x}Ge_x$:H films initially nucleate

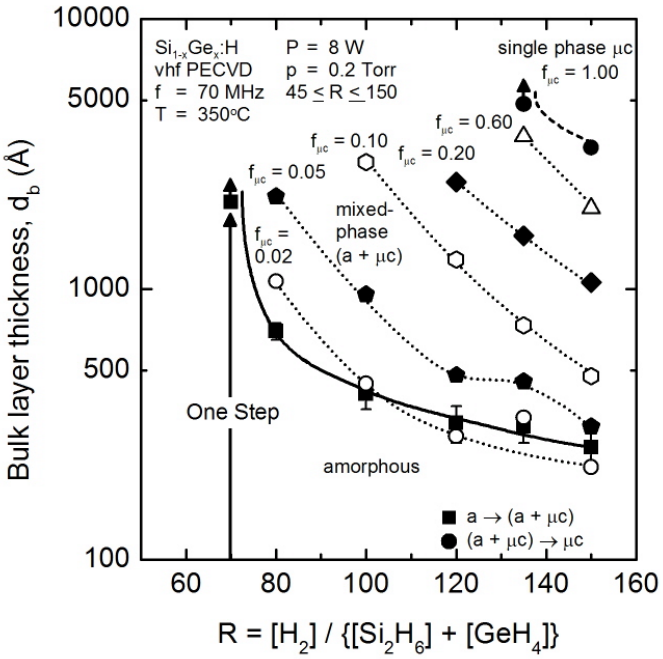

Figure 5. A deposition phase diagram for $Si_{1-x}Ge_x$:H films prepared under vhf PECVD conditions with G=0.286. The bulk layer thicknesses at which the a → (a+μc) transition (solid line, squares), and the (a+μc) → μc transition (dashed line, closed circles) occur are depicted, as deduced from the surface roughness evolution. Up-arrows indicate that the transitions occur at thicknesses above the indicated values. Contour lines in the microcrystallite fraction $f_{\mu c}$ are plotted ranging from 0.02 to 0.60 (dotted lines). The surface roughening effect provides sensitivity to the a → (a+μc) transition at microcrystalline volume fractions of ~0.01-0.03 within the near-surface of the bulk layer.

on the underlying n-layer as a-$Si_{1-x}Ge_x$:H but, as in the case of Si:H, undergo the a → (a+μc) transition at a thickness that decreases with increasing R. Figure 5 shows that the a → (a+μc) transition as observed in the surface roughness thickness evolution is sensitive to microcrystalline volume fractions of <0.02 in the near-surface of the bulk layer at low R, but the sensitivity degrades at higher R as the a → (a+μc) transition shifts to lower thickness.

The n-i structures co-deposited on the textured Ag/ZnO back-reflectors from the two series of Figs. 1-5 (including additional films in which the depositions were terminated at ~2000 Å) were then fabricated into solar cells and characterized to extract the open circuit voltage (V_{oc}), short circuit current (J_{sc}), fill factor (FF), and efficiency (η). Results for a-Si:H with G=0 and for the alloys with G=0.286 are given in Figs. 6 and 7, respectively, and will be discussed next.

DISCUSSION

The vhf PECVD phase diagrams of Figs. 4 and 5 have been developed with the intent of optimizing systematically the top and middle i-layers of triple junction n-i-p solar cells. Toward this goal, i-layers of these two series have been incorporated into single-junction devices with bulk layer thicknesses of ~2000 Å and with 25°C Tauc gaps of ~1.8 eV and ~1.5 eV for the top and middle i-layers, respectively. The diagrams of Figs. 4 and 5 provide insights into how these Si:H and $Si_{1-x}Ge_x$:H films evolve with thickness at different H_2 dilution levels. In fact, the diagrams for vhf PECVD from Si_2H_6+GeH_4 show all the features characteristic of previous diagrams for films from SiH_4+GeH_4. Thus, by understanding the nature of microcrystallite evolution and quantifying the phase composition as in Figs. 4 and 5, it may be possible to select H_2 dilution levels in order to maximize film quality for one-step, multi-step, or graded layers.

In the case of a 2000 Å thick a-Si:H i-layer, the optimum one-step deposition process is predicted on the basis of the phase diagram to occur at the maximal value of R = 80, i.e., the largest R possible such that the i-layer remains amorphous throughout its thickness during growth. This prediction is borne out in the device performance. At R=100 the a → (a+μc) transition occurs at 600 Å, however, and the microcrystalline fraction in the near-surface of the 2000 Å i-layer is ~ 0.09. The Si:H crystallites appear to degrade V_{oc} significantly due to their

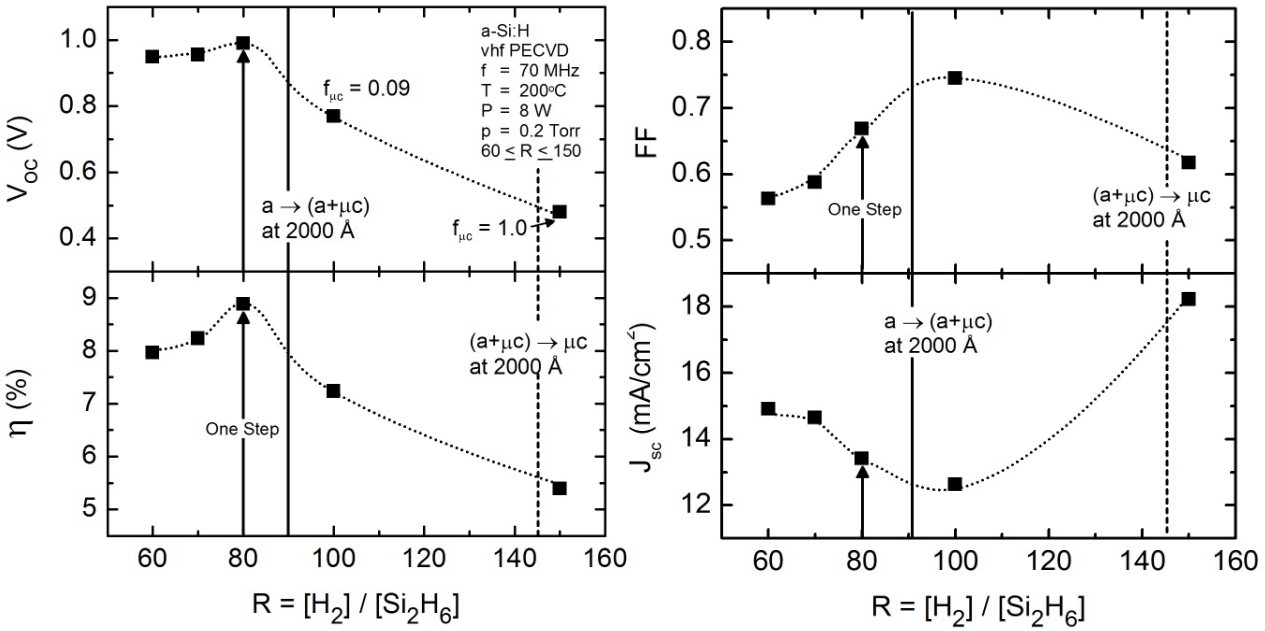

Figure 6 (above). Device characteristics for single-junction n-i-p solar cells deposited on textured back-reflectors in which the i-layers are pure Si:H films prepared by vhf PECVD. The open circuit voltage (V_{oc}, upper left), efficiency (η, lower left), fill factor (FF, upper right), and short circuit current (J_{sc}, lower right) are plotted versus the R value of the i-layer.

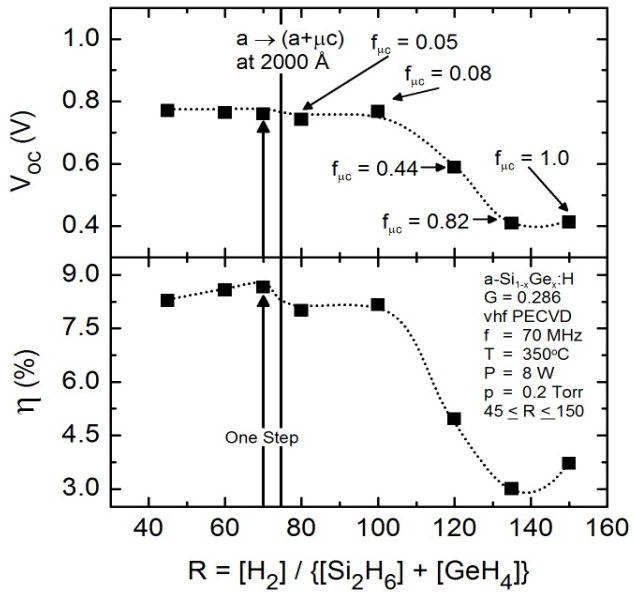

Figure 7 (right). Device characteristics for single-junction n-i-p solar cells deposited on textured back-reflectors in which the i-layers are $Si_{1-x}Ge_x$:H. The open circuit voltage (V_{oc}, upper) and efficiency (η, lower) are plotted versus the R value of the i-layer.

presence at the i/p interface. The one-step optimized process for a 2000 Å thick a-$Si_{1-x}Ge_x$:H i-layer is expected at R = 70 according to the same principle, and this optimum is also borne out in the devices, but less distinctly. Above R=70 a detectable volume fraction of microcrystalline $Si_{1-x}Ge_x$:H is present in the near-surface of the film ranging from 0.05 at R = 80 to 0.08 at R=100. In contrast to Si:H, the presence of the microcrystallites at the i/p interface of the $Si_{1-x}Ge_x$:H solar cells does not significantly decrease V_{oc} and efficiency. Although the overall performance of the devices remains acceptable for $70 < R \leq 100$ in Fig. 7, this region is avoided due to irreproducibility, including a dependence on the underlying n-layer structure and poor yield. Next V_{oc} and FF will be discussed further with strategies for multistep improvements.

Considering first the variation in V_{oc} for Si:H, this parameter increases with increasing R for i-layers below the optimum at R=80 due to the increase in band gap; however, a more abrupt increase occurs that defines the optimum as the a → (a+μc) transition is approached. This is the

protocrystalline regime, characterized by an improvement in ordering as well as an increase in band gap. Because V_{oc} is strongly influenced by the film properties at the very top of the i-layer, there is an abrupt decrease in its value above R=80 due to the presence of crystalline nuclei at the top of the film. When the top of the film is mixed-phase Si:H, V_{oc} lies between the values for protocrystalline Si (~ 1 eV) and μc-Si:H (~0.5 eV). For R values above the (a+μc) → μc transition for a 2000 Å thick film, a V_{oc} value appropriate for μc-Si:H is expected. In contrast, V_{oc} for $Si_{1-x}Ge_x$:H shows only a weak dependence on R throughout the amorphous growth regime and even across the a → (a+μc) transition. In this case, the effect of R on the optical band gap of $Si_{1-x}Ge_x$:H is also weaker. The lack of a strong effect of the i/p interface crystallites for $Si_{1-x}Ge_x$:H may be due to the fact that over a wide range of R the microcrystallites do not appear to grow preferentially as cone-like structures as in Si:H, but rather as isolated clusters.

The behavior of the fill factor (FF) with R for both Si:H and $Si_{1-x}Ge_x$:H suggests the possibility of an improvement in the cell performance with multistep processing. As an example, Fig. 6 shows that, although the FF increases with R, its maximum of 0.74 is reached at an R value larger than that maximizing V_{oc}. Because the FF is controlled predominantly by the bulk i-layer, the presence of a small volume fraction of crystallites at the i/p interface that reduces V_{oc} does not adversely affect the FF. The FF actually seems to benefit from the incorporation of microcrystallites in the bulk of the Si:H; however, the improvement may in fact be due to improvements in the amorphous material when it is deposited with increasing R from 80 to 100 (i.e., increases in the band gap and protocrystalline ordering). One may be able to take advantage of an optimum V_{oc} and FF simultaneously by depositing the bulk (~1800 Å) of the i-layer with R=100, then depositing a thin (< 100 Å) substrate-memory-erasing low R layer -- similar to the starting n-layer, before finally completing the cell with a second ~200 Å R=100-120 layer. The key, however, is to ensure that the memory-erasing layer first is successful at suppressing the continued growth of crystallites, and second is not detrimental to the FF.

SUMMARY

Deposition phase diagrams have been developed and augmented for vhf PECVD of thin film Si:H and its alloys with Ge by incorporating contour lines representing the crystalline fraction in the top ~10 Å of the i-layer at a given bulk layer thickness. These diagrams predict optimum one-step i-layer deposition processes for the top and middle cells of a triple-junction device that are in consistency with the performance of single-junction devices. V_{oc} and FF appear to be optimized at different values of R suggesting that a multistep PECVD process may be beneficial.

ACKNOWLEDGMENTS

This research was supported by NREL (Subcontract No. RXL-5-44205-06).

REFERENCES

[1] J. Yang, A. Banerjee, and S. Guha, *Appl. Phys. Lett.* **70,** 2975 (1997).

[2] X. Deng, X.B. Liao, S.J. Han, H. Povolny, and P. Agarwal, *Solar Energy Mater. Solar Cells* **62**, 89 (2000).

[3] D.V. Tsu, B.S. Chao, S.R. Ovshinsky, S. Guha, and J. Yang, *Appl. Phys. Lett.* **71**, 1317 (1997).

[4] R.W. Collins and A.S. Ferlauto, *Curr. Opinion Solid State Mater. Sci.* **6**, 425 (2002).

[5] I. An, J.A. Zapien, C. Chen, A.S. Ferlauto, A.S. Lawrence, and R.W. Collins, *Thin Solid Films* **455**, 132 (2004).

[6] P. Lautenschlager, M. Garriga, L. Viña, and M. Cardona, *Phys. Rev. B* **36**, 4821 (1987).

[7] A.S. Ferlauto, G.M. Ferreira, J.M. Pearce, C.R. Wronski, R.W. Collins, G. Ganguly, and X. Deng, *J. Appl. Phys.* **92**, 2424 (2002).